

Collapsing D-branes in one-parameter models and small/large radius duality

C. I. Lazaroiu¹

Department of Physics
Columbia University
New York, N.Y. 10027

ABSTRACT

We finalize the study of collapsing D-branes in one-parameter models by completing the analysis of the associated hypergeometric hierarchy. This brings further evidence that the phenomenon of collapsing 6-branes at the mirror of the ‘conifold’ point in IIA compactifications on one-parameter Calabi-Yau manifolds is generic. It also completes the reduction of the study of higher periods in one-parameter models to a few families which display characteristic behaviour. One of the models we consider displays an exotic form of small-large radius duality, which is a consequence of an “accidental” discrete symmetry of its moduli space. We discuss the implementation of this symmetry at the level of the associated type II string compactification and its action on D-brane states. We also argue that this model admits two special Lagrangian fibrations and that the symmetry can be understood as their exchange.

¹ lazaroiu@phys.columbia.edu

Introduction

Recent work on “D-brane geometry” [21] has led to renewed interest in the quantum analogue of the notion of ‘size’. A necessary preliminary of analyses such as [20] is the identification of those D-brane states which become massless at special points in the moduli space of a type II compactification on a Calabi-Yau manifold, which in the language of [16, 1] amounts to identifying the cycles which acquire zero quantum volume at such a point. Many basic questions in quantum geometry still await an answer, one of the most important among these being the central issue of marginal stability and its implications for the extension of mirror symmetry to the D-brane sector of compactified string theory. Such an extension holds promise of providing a tool for understanding quantum corrections to the moduli space of type IIA BPS saturated D-branes. Progress along these lines should enable us to understand the tantalizing conjectures of [11] and [10].

One of the obstacles to a detailed and reasonably general investigation of D-brane effects in $N = 2$ string compactifications is the difficulty of performing computations of a basis of periods of the holomorphic 3-form *throughout* the complex structure moduli space of a given Calabi-Yau manifold. In [1], we took a few steps towards removing this obstacle, at least in the one-parameter case, by showing how the largely overlooked¹ but classical technique of Meijer functions [24, 27] can be used to give a systematic approach to the problem. In fact, this technique allows us to reduce most one-parameter models to four classes, each of which allows for universal expressions of a special set of periods introduced in [1]. Determining the analytic continuation of periods for all such classes amounts to a complete solution of the problem — given a one parameter model, all that remains to be done is to substitute in these expressions for the specific values of the hypergeometric parameters. In [1] we made use of this approach in order to undertake a systematic study of quantum volumes in one parameter models and along a special sub-locus of a two-parameter example. Considerations of space prevented us from giving a complete discussion of all classes of one-parameter models. The present paper remedies this lack of completeness by carrying through a similar analysis for the last two classes of this hierarchy, which in a certain sense are the most degenerate situations. This allows us to bring further evidence that the phenomenon noticed in [16, 9] of collapsing 6-branes at the mirror of the conifold point is generic in one-parameter models, and not limited to the case of the quintic [19], where it was first observed.

The last part of the paper is concerned with a special example which exhibits some rather exotic features. This is a one-parameter family of Calabi-Yau complete intersections in seven-dimensional projective space, which belongs to the most “degenerate” family in our classification. As noticed a while ago [18], the moduli space of this model admits a \mathbb{Z}_2 symmetry which identifies the small and large radius limits. This lead

¹An example in which Meijer functions were used for performing the analytic continuation of periods can be found in [2]. We thank Erik Zaslow for bringing this reference to our attention.

to suspicions [23] that the model provides a Calabi-Yau example of small-large radius duality. This would give an example of a ‘T-dual’ string compactification with reduced ($N=2$) supersymmetry, with potentially interesting implications for phenomenology. Our knowledge of a basis of periods allows us to address some of the puzzles concerning this model. While doing so in Section 3, we will meet with some surprises. Indeed, we will be able to confirm the suspicions of [23], but in a rather unexpected way: while small-large radius duality is indeed an exact feature of the model, its realization involves a certain rotation in the space of states, as well as a (less surprising) rescaling of the correlation functions. This conclusion, which can be extracted from the direct computation of periods by a careful consideration of branch cuts, has some interesting implications for the action of the symmetry on the D-brane states. In particular, the duality exchanges D2 and D4-branes in the mirror, type IIA compactification. In Section 5, we propose an explanation of this phenomenon by making use of the ideas of Strominger, Yau and Zaslow [32]. We will argue that the model admits *two* T^3 fibrations, which are interchanged by our symmetry. The nontrivial action on D2/D4 branes appears as a consequence of the fact that the dimension of the holomorphic cycle wrapped by the mirror of a given type IIB D-brane depends on the position of the original special Lagrangian cycle with respect to the fibration: when changing the fibration, the interpretation of the mirror state is modified. The existence of this symmetry has other interesting implications for the D-brane physics of this model. In particular, there exists a two-dimensional space of D-brane states which vanish at the mirror of the “conifold” point (modulo issues of marginal stability). Such states can be interpreted as composites of D4 and D6 branes.

1 Quantum notions of “size”

The problem of understanding the correct string-theoretic generalization of the notion of size was considered in [44, 45, 16] (see also [1] for a review). The best framework for addressing this issue is that of type II string compactifications on Calabi-Yau manifolds, which have the advantage of allowing for exact computations of stringy corrections while at the same time displaying nontrivial quantum effects. This problem can be approached by considering a type IIA compactification on a Calabi-Yau manifold X and its dual, type IIB compactification on the mirror Y of X . The quantum corrections to the notion of size appear in the vector multiplet moduli space, which corresponds to the Kahler moduli of the IIA compactification and to the complex structure moduli of its IIB dual. Since the latter does not suffer quantum corrections [46], one can use mirror symmetry in order to transport the results accessible on this side to the IIA compactification, thereby extracting exact information about the stringy corrections to the Kahler moduli space of X . Hence mirror symmetry identifies the quantum-corrected complexified Kahler moduli space of X with the complex structure moduli space \mathcal{M} of Y .

The first question one encounters in this framework is that of introducing a physi-

cally meaningful parameterization of the corrected complexified Kahler moduli space, which will allow us to measure ‘quantum areas’ on X . In this paper, we will follow the proposal of [44], which consists of using the value of the complexified Kahler class dictated by the mirror map:

$$k(z) = (B + iJ)(z) = \frac{\int_{\gamma_1} \Omega(z)}{\int_{\gamma_0} \Omega(z)} \ , \quad (1)$$

where z is a coordinate² on \mathcal{M} , Ω is the holomorphic 3-form of Y and γ_0, γ_1 are certain 3-cycles in Y which can be identified in the manner discussed in [19, 14, 25, 30, 29]. Hence (1) defines a specific class in $H^2(X, \mathbb{C})$ at each point z , which is identified as the correct quantum counterpart of the complexified Kahler class at that point. The imaginary part J of this class defines the so-called ‘nonlinear sigma model measure’ on \mathcal{M} . More precisely, writing:

$$k(z) = t(z)e \ , \quad (2)$$

where e is the generator of $H^2(X, \mathbb{Z})$ defines a special coordinate on \mathcal{M} (in the sense of special geometry). Then the nonlinear sigma model measure is defined by the imaginary part of $t(z)$.

An ‘intermediate’ parameterization of \mathcal{M} is given by the so-called ‘algebraic coordinate’, which is defined through:

$$k_{alg} = (b + is)(z) = \frac{1}{2\pi i} \log(\kappa z)e \ , \quad (3)$$

where κ is a certain constant which is determined by the monomial -divisor mirror map of [13]. Measuring distances with k_{alg} amounts to using the semiclassical notion of size (which is, strictly speaking, only valid in the large radius limit of X) throughout the entire moduli space \mathcal{M} .

An important point, first noticed in [16] and discussed in full generality in [1] is that the classical geometric relation:

$$\text{vol}(\Sigma_{2p}) \sim \int_{\Sigma_{2p}} k^p \quad (4)$$

(with Σ_{2p} some 2p-cycle in X) does not admit a natural generalization to the quantum level. This follows by noticing that the most natural extension of the notion of volume to the quantum setting is to identify the ‘quantum volume’ of Σ_{2p} with the mass of a D_{2p} brane wrapping this cycle (divided by the associated D-brane tension). This can be computed via mirror symmetry techniques in the BPS case (when Σ_{2p} is a holomorphic cycle and hence the associated D-brane state is BPS), since the mass of the mirror state (a type IIB $D3$ -brane wrapping a special Lagrangian 3-cycle C mirror to Σ_{2p}) is given by the exact formula:

$$m(C) = \frac{|\int_C \Omega|}{|\int_C \bar{\Omega} \wedge \Omega|^{1/2}} = m(\Sigma_{2g}) \ . \quad (5)$$

²We restrict to one-parameter models for simplicity.

The disagreement between quantum volumes measured in this way and those given by (4) is due to open string instanton corrections³ to the mass of the corresponding D_{2p} brane [17]. In fact, using the semiclassical relation (4) amounts to substituting the correct quantum Kahler class into the *classical* relation for volumes—a procedure somewhat akin to using the algebraic measure (3) instead of the correct, nonlinear sigma model measure.

An important question raised by these considerations is to what extent this notion of quantum volume behaves like its geometric counterpart. Since the definition discussed above includes nontrivial quantum corrections from open string instantons, it is natural to expect that the two quantities will diverge as we move away from the large radius limit of X into regions of the moduli space where such corrections are important. In fact, instanton corrections are especially strong in the vicinity of conifold points, so one expects that the most pronounced difference will be manifest there. This suspicion is confirmed by the observation of [16, 9] that the quantum volume of IIA $D2$ and $D4$ branes on the quintic remains nonzero at the mirror of the conifold point, while the quantum volume of a $D6$ -brane vanishes. In [1], we presented evidence that this is a widespread phenomenon in Calabi-Yau compactifications, and not a peculiarity of the quintic. However, the analysis of [1] was limited to only two of the four hypergeometric families of one parameter models. The purpose of next three sections is to complete this argument, by showing that the same behaviour occurs in the remaining families, thus providing more evidence that this is a generic feature of one-parameter compactifications.

Most of the results of the next three sections are of a somewhat technical nature and represent a direct extension of the work of [1]. The reader mainly interested in the discussion of Calabi-Yau small-large radius duality can proceed directly to Section 5.

2 Universal results for one-parameter models

This section reviews and completes some results obtained in [1], which will be used intensively below. These rest on the theory of Meijer functions [24, 27], a brief account of which can be found in [1].

2.1 Review of large radius results

Let us start by summarizing some material presented in [1]. Following the discussion of that paper, we focus on one-parameter models whose hypergeometric symbol has the form $\left(\begin{smallmatrix} \alpha_1, \alpha_2, \alpha_3, \alpha_4 \\ 1, 1, 1 \end{smallmatrix} \right)$ with α_j some rational numbers contained in the interval $[0, 1]$. In this case, the associated Picard-Fuchs equation has the hypergeometric form:

$$\left[\delta^4 - z(\delta + \alpha_1)(\delta + \alpha_2)(\delta + \alpha_3)(\delta + \alpha_4) \right] u = 0 \quad (6)$$

³These are induced by open strings whose endpoints are constrained to lie in Σ_{2p} .

(where $\delta := z \frac{d}{dz}$). By using the theory of Meijer functions, it was shown in [1] that an especially convenient basis of periods (called *Meijer periods*) is given by the integral representations:

$$U_j(z) = \frac{1}{2\pi i} \int_{\gamma} ds \phi_j(s) , \quad (7)$$

where:

$$\phi_j(s) := \frac{1}{\prod_{i=1 \dots 4} \Gamma(\alpha_i)} \frac{\Gamma(-s)^{j+1} \prod_{i=1 \dots 4} \Gamma(s + \alpha_i)}{\Gamma(s+1)^{3-j}} ((-1)^{j+1} z)^s . \quad (8)$$

In these expressions, the contour γ is chosen as shown in Figure 1.

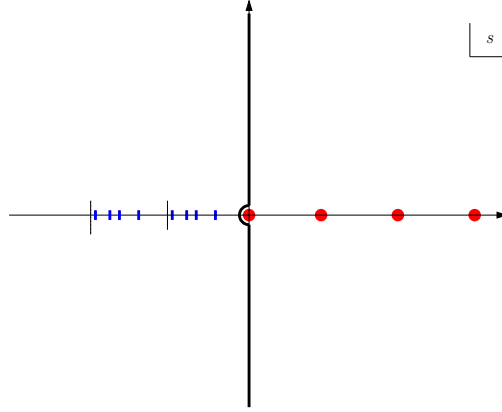


Figure 1. The defining contour for the Meijer periods.

The expansions of these periods in the large and small radius regions of the moduli space follow by closing the contour to the right or left, which is allowed for $|z| < 1$ and $|z| > 1$ respectively. The expansions for $|z| < 1$ were computed in [1] and are given by the universal expression:

$$U_j(z) = \frac{(-1)^j}{j!} \sum_{n=0}^{\infty} \frac{(\alpha_1)_n (\alpha_2)_n (\alpha_3)_n (\alpha_4)_n}{n!^4} \nu_j(n, z) z^n , \quad (9)$$

where:

$$\begin{aligned} \nu_0 &= 1 \\ \nu_1(n, z) &= g'_1(n, z) = \eta_1(n) + \log(z) \\ \nu_2(n, z) &= g''_2(n, z) + [g'_2(n, z)]^2 = \eta'_2(n) + (\eta_2(n) + \log(-z))^2 \\ \nu_3(n, z) &= g'''_3(n, z) + 3g''_3(n, z)g'_3(n, z) + g'_3(n, z)^3 = \eta''_3(n) + 3\eta'_3(n)(\eta_3(n) + \log z) + (\eta_3(n) + \log z)^3 , \end{aligned} \quad (10)$$

with:

$$\eta_j^{(i)}(n) = \sum_{k=1}^4 \psi^{(i)}(n + \alpha_k) - (3-j)\psi^{(i)}(n+1) - (-1)^i(j+1) \left[\psi^{(i)}(1) + i! \sum_{l=1}^n \frac{1}{l^{i+1}} \right] , \quad (11)$$

for $i = 0, 1, 2$. In [1], we also computed the monodromy matrix of the Meijer periods about the large complex structure point $z = 0$, with the result:

$$T[0] = \begin{bmatrix} 1 & 0 & 0 & 0 \\ -2i\pi & 1 & 0 & 0 \\ -4\pi^2 & -2i\pi & 1 & 0 \\ 0 & 0 & -2i\pi & 1 \end{bmatrix} . \quad (12)$$

2.2 The special coordinate on the moduli space

For later use, let us derive a universal expression for the special coordinate t on the moduli space. As explained in [14, 30, 25, 29, 13], this is given by a certain ratio of a linear combination of \log^0 and \log^1 periods to a \log^0 period (the latter is, of course, determined up to a global factor). The correct linear combination appearing in the numerator is fixed by the requirement that the asymptotic form of t in the large complex structure limit be given by:

$$t_{as} = \frac{1}{2\pi i} \log w , \quad (13)$$

where $w = \kappa z$, with $\kappa = e^{\sum_{k=1}^4 \psi(\alpha_k) - 4\psi(1)}$, is a coordinate on the moduli space determined by the monomial-divisor mirror map of [13]. The asymptotic form of the Meijer periods at large complex structure can be easily extracted from the expansions in terms of w computed in [1]. Indeed, it was shown there that (9) can be rewritten as:

$$U_j(w) = \sum_{s=0}^j \tilde{q}_{sj}(w) (\log w)^s , \quad (14)$$

where:

$$\tilde{q}_{sj}(w) := \frac{(-1)^j}{j!} \sum_{n=0}^{\infty} \frac{(\alpha_1)_n (\alpha_2)_n (\alpha_3)_n (\alpha_4)_n}{n!^4} \tilde{v}_{sj}(n) \left(\frac{w}{\kappa} \right)^n , \quad (15)$$

with $\tilde{v}_{sj}(n)$ some quantities whose explicit form is listed in Subsection 4.2.1 of [1]. Since the matrix $\tilde{q}(0) := (q_{sj}(0))_{s,j=0..3}$ has a finite limit at $w = 0$,

$$\tilde{q}(0) := \begin{bmatrix} 1 & 0 & \frac{1}{2}(\eta_2'(0) - \pi^2) & -\frac{1}{6}\eta_3''(0) \\ 0 & -1 & i\pi & -\frac{1}{2}\eta_3'(0) \\ 0 & 0 & \frac{1}{2} & 0 \\ 0 & 0 & 0 & -\frac{1}{6} \end{bmatrix} , \quad (16)$$

it follows that the leading terms in the large radius expansions of the Meijer periods are:

$$U_j^{as}(w) = \sum_{s=0}^j \tilde{q}_{sj}(0)(\log w)^s . \quad (17)$$

In particular, we obtain:

$$U_0^{as}(w) = 1 \quad , \quad U_1^{as}(w) = -\log w \quad (18)$$

and since the periods U_j are adapted to the monodromy weight filtration of the model we immediately deduce that the special coordinate has the simple universal form:

$$t = -\frac{1}{2\pi i} \frac{U_1}{U_0} . \quad (19)$$

Substituting expansion (9) in this formula leads to a general expression for the special coordinate in the large radius region $|z| < 1$ (which can be used, in particular, to extract *universal* expressions for the Gromov-Witten invariants [5, 6] of this class of models as functions of the parameters α_k). On the other hand, the analytic continuations of U_0 and U_1 allow us to compute t as a function of z (or w) throughout the moduli space.

2.3 The hypergeometric hierarchy

As discussed in [1], the nature of the small radius expansions of the Meijer periods, and hence the nature of the small radius point of the model, depend on the relative values of the parameters α_i . From an abstract point of view, this leads to a hierarchy of models characterized (up to permutations of α_i) by one of the conditions:

- (0) all α_i are distinct
- (1) three of the parameters α_i are distinct
- (2) $\alpha_1 = \alpha_2$ and $\alpha_3 = \alpha_4$ but $\alpha_1 \neq \alpha_3$
- (3) $\alpha_1 = \alpha_3 = \alpha_3 = \alpha_4$.
- (4) $\alpha_1 = \alpha_2 = \alpha_3 \neq \alpha_4$

Only levels (0), (1), (2) and (3) of this hierarchy are realized through one-parameter complete intersections in projective spaces, as well as through many one-parameter complete intersections in weighted projective spaces and more general toric varieties (see [15] for a discussion of toric geometry). Level (4) does not seem to be realized⁴ through compact one-parameter complete intersections in toric varieties, though it could be realized through more general constructions. Since we are mostly interested in the toric case, we will limit ourselves to the families (0), (1), (2) and (3). A few examples of models belonging to these classes are listed in Table 1.

⁴This follows from the results of [31].

<i>Family</i>	<i>Model</i>	$(\alpha_1, \alpha_2, \alpha_3, \alpha_4)$
0	$\mathbb{P}^4[5]$	$(1/5, 2/5, 3/5, 4/5)$
0	$\mathbb{WP}^{2,1,1,1,1}[6]$	$(1/3, 2/3, 1/6, 5/6)$
0	$\mathbb{WP}^{4,1,1,1,1}[8]$	$(1/8, 3/8, 5/8, 7/8)$
0	$\mathbb{WP}^{5,2,1,1,1}[10]$	$(1/10, 3/10, 7/10, 9/10)$
0	$\mathbb{WP}^{2,1,1,1,1,1}[3,4]$	$(1/3, 2/3, 1/4, 3/4)$
0	$\mathbb{WP}^{3,2,2,1,1,1}[4,6]$	$(1/6, 1/4, 3/4, 5/6)$
1	$\mathbb{P}^5[2,4]$	$(1/2, 1/2, 1/4, 3/4)$
1	$\mathbb{P}^6[2,2,3]$	$(1/2, 1/2, 1/3, 2/3)$
1	$\mathbb{WP}^{3,1,1,1,1,1}[2,6]$	$(1/2, 1/2, 1/6, 5/6)$
2	$\mathbb{P}^5[3,3]$	$(1/3, 1/3, 2/3, 2/3)$
2	$\mathbb{WP}^{2,2,1,1,1,1}[4,4]$	$(1/4, 1/4, 3/4, 3/4)$
2	$\mathbb{WP}^{3,3,2,2,1,1}$	$(1/6, 1/6, 5/6, 5/6)$
3	$\mathbb{P}^7[2,2,2,2]$	$(1/2, 1/2, 1/2, 1/2)$

Table 1. Some examples of models belonging to various hypergeometric families.

In [1], we studied only the families (0) and (1). Here we consider the more degenerate families (2) and (3). As we show below, these models can also be approached efficiently by the general methods developed in [1]. The highly degenerate family (3) displays some surprising, which we discuss in detail in Section 5.

2.4 The choice of branch-cuts

Let us clarify the choice of branch-cuts used in the present paper and implicitly in [1]. Our convention is that we start from the large complex structure region $|z| < 1$ and perform the analytic continuation through the sector $\arg(z) \in (-\pi, 0)$, i.e. through the lower half of the unit circle in the complex plane (see Figure 2). Moreover, we will pick the branch-cut of all periods to lie along the negative real axis $(-\infty, 0)$. With this convention, expressions such as $\log(-z)$, $\log(-1/z)$ and $\log(z)$ are always understood to have the cut on the negative real axis, so that we can write:

$$\log(-z) = \log(z) + i\pi \quad , \quad \log(-1/z) = -\log(z) - i\pi \quad . \quad (20)$$

A similar convention is used for power functions with non-integral exponents. In particular, we have $(-z)^{-\alpha} = z^\alpha e^{-i\pi\alpha}$ for any real constant α . For the ‘generic’ model considered in [1] the branch-cut along $(-\infty, 0)$ suffices for all periods. For the other families (and in particular for all models discussed in the present paper), the situation is slightly different since in these cases the analytic continuation of the fundamental period U_0 displays logarithmic behaviour in the region $|z| > 1$, even though it is regular in the unit disk, $|z| < 1$. This requires that we enlarge the associated branch-cut in a way consistent with this behaviour, and we shall do so by adding the upper half of the unit circle to the common cut along the negative real axis.

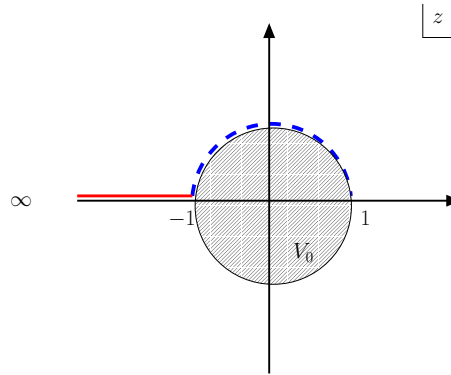


Figure 2. Our choice of branch-cuts for the analytic continuation of periods. The upper half of the unit circle is added only for the fundamental period U_0 , in all cases when this period displays logarithmic behaviour in the region $|z| > 1$.

3 The family $\alpha_1 = \alpha_2, \alpha_3 = \alpha_4$

Consider first the family (2), which corresponds to the hypergeometric symbol $\left(\begin{matrix} \alpha, \alpha, \beta, \beta \\ 1, 1, 1 \end{matrix} \right)$, i.e. to the parameters $\alpha_1 = \alpha_2 := \alpha, \alpha_3 = \alpha_4 := \beta$ with $\alpha \neq \beta$, where we take $0 < \alpha, \beta < 1$.

3.1 The Meijer periods

The expansion of the Meijer periods for $|z| < 1$ follows by substituting our particular values for α_i in the general formula (9). The expansions for $|z| > 1$ follow by closing the contour to the right, which gives contributions from the B-type poles:

$$(B_1) \quad s = -n - \alpha$$

$$(B_2) \quad s = -n - \beta$$

(with n a nonnegative integer). Noticing that all such poles are double, a straightforward residue computation yields:

$$U_j(z) = \left(\frac{\sin \pi \alpha}{\pi} \right)^{3-j} ((-1)^{j+1} z)^{-\alpha} \sum_{n=0}^{\infty} \frac{\Gamma(n+\alpha)^4 \Gamma(-n+\beta-\alpha)^2}{\Gamma(\alpha)^2 \Gamma(\beta)^2 n!^2} z^{-n} \times$$

$$\left[2\psi(1) + 2\psi(-n+\beta-\alpha) - (j+1)\psi(n+\alpha) - (3-j)\psi(-n-\alpha+1) + 2 \sum_{k=1}^n \frac{1}{k} + \log((-1)^{j+1} z) \right] \quad (21)$$

$$+(\alpha \longleftrightarrow \beta) .$$

3.2 Meijer monodromies

The monodromy of the Meijer basis about $z = 0$ follows by applying the results reviewed above, while the monodromy about $z = \infty$ can be computed by making use of the general techniques developed in [1]. Following that procedure, we first determine the canonical and Jordan forms of the matrix $R[\infty]$:

$$R_{can}[\infty] = \begin{bmatrix} 0 & -1 & 0 & 0 \\ 0 & 0 & -1 & 0 \\ 0 & 0 & 0 & -1 \\ \alpha^2 \beta^2 & -2\alpha^2 \beta - 2\alpha \beta^2 & \alpha^2 + 4\alpha \beta + \beta^2 & -2\alpha - 2\beta \end{bmatrix}, \quad R_J[\infty] = \begin{bmatrix} -\beta & 1 & 0 & 0 \\ 0 & -\beta & 0 & 0 \\ 0 & 0 & -\alpha & 1 \\ 0 & 0 & 0 & -\alpha \end{bmatrix} .$$

The relation $R_{can}[\infty] = P R_J[\infty] P^{-1}$ allows us to determine a choice for the transition matrix P from a Jordan basis to the canonical basis:

$$P = \begin{bmatrix} \frac{\alpha^2 \beta}{\alpha^2 - 2\alpha \beta + \beta^2} & \frac{(\alpha - 3\beta)\alpha^2}{\alpha^3 - 3\alpha^2 \beta + 3\alpha \beta^2 - \beta^3} & \frac{\alpha \beta^2}{\alpha^2 - 2\alpha \beta + \beta^2} & \frac{(3\alpha - \beta)\beta^2}{\alpha^3 - 3\alpha^2 \beta + 3\alpha \beta^2 - \beta^3} \\ \frac{\alpha^2 \beta^2}{\alpha^2 - 2\alpha \beta + \beta^2} & -2 \frac{\alpha^2 \beta^2}{\alpha^3 - 3\alpha^2 \beta + 3\alpha \beta^2 - \beta^3} & \frac{\alpha^2 \beta^2}{\alpha^2 - 2\alpha \beta + \beta^2} & 2 \frac{\alpha^2 \beta^2}{\alpha^3 - 3\alpha^2 \beta + 3\alpha \beta^2 - \beta^3} \\ \frac{\beta^3 \alpha^2}{\alpha^2 - 2\alpha \beta + \beta^2} & - \frac{\alpha^2 \beta^2 (\alpha + \beta)}{\alpha^3 - 3\alpha^2 \beta + 3\alpha \beta^2 - \beta^3} & \frac{\alpha^4 \beta^2}{\alpha^2 - 2\alpha \beta + \beta^2} & 2 \frac{\alpha^3 \beta^3}{\alpha^3 - 3\alpha^2 \beta + 3\alpha \beta^2 - \beta^3} \end{bmatrix} . \quad (22)$$

In the present case, the singular content of the periods around $z = \infty$ can be extracted by writing $U^t(z) = Z(z)q(z)$, where $Z(z) = [z^{-\alpha} \quad z^{-\alpha} \log z \quad z^{-\beta} \quad z^{-\beta} \log z]$ and $q(z) = (q_{sj}(z))_{s,j=0..3}$, with:

$$q_{0j}(z) = (\delta_{j,odd} + \delta_{j,even} e^{i\pi\alpha}) \left(\frac{\sin \pi \alpha}{\pi} \right)^{3-j} \sum_{n=0}^{\infty} \frac{\Gamma(n+\alpha)^4 \Gamma(-n+\beta-\alpha)^2}{\Gamma(\alpha)^2 \Gamma(\beta)^2 n!^2} z^{-n} \times$$

$$\left[2\psi(1) + 2\psi(-n+\beta-\alpha) - (j+1)\psi(n+\alpha) - (3-j)\psi(-n-\alpha+1) + 2 \sum_{k=1}^n \frac{1}{k} + i\pi \delta_{j,even} \right]$$

$$q_{1j}(z) = (\delta_{j,odd} + \delta_{j,even} e^{i\pi\alpha}) \left(\frac{\sin \pi \alpha}{\pi} \right)^{3-j} \sum_{n=0}^{\infty} \frac{\Gamma(n+\alpha)^4 \Gamma(-n+\beta-\alpha)^2}{\Gamma(\alpha)^2 \Gamma(\beta)^2 n!^2} z^{-n} ,$$

and $q_{2j}(z) = q_{0j}(z)|_{\alpha \leftrightarrow \beta}$, $q_{3j}(z) = q_{1j}(z)|_{\alpha \leftrightarrow \beta}$.

On the other hand, the matrix $z^{R_J[\infty]}$ has the simple form:

$$z^{R_J[\infty]} = \begin{bmatrix} z^{-\beta} & \ln(z)z^{-\beta} & 0 & 0 \\ 0 & z^{-\beta} & 0 & 0 \\ 0 & 0 & z^{-\alpha} & \ln(z)z^{-\alpha} \\ 0 & 0 & 0 & z^{-\alpha} \end{bmatrix}. \quad (23)$$

This allows us to find the matrix $q_J(z)$ which satisfies $U_J^t(\infty) = Z(z)q_J(z)$:

$$q_J(z) = \begin{bmatrix} 0 & 0 & S_{1,3}(z) & S_{1,4}(z) \\ 0 & 0 & 0 & S_{1,3}(z) \\ S_{1,1}(z) & S_{1,2}(z) & 0 & 0 \\ 0 & S_{1,1}(z) & 0 & 0 \end{bmatrix}. \quad (24)$$

In this expression, $S_{ij}(z)$ are the entries of the matrix $S(z)$ which defines the nilpotent orbit of the fundamental system $\Phi_J(z)$ associated with the Jordan basis $U_J(z)$:

$$\Phi_J(z) = S(z)z^{R_J}. \quad (25)$$

Since $S(\infty) = P$, we obtain:

$$q_J(\infty) = \begin{bmatrix} 0 & 0 & \frac{\alpha\beta^2}{(-\beta+\alpha)^2} & \frac{(3\alpha-\beta)\beta^2}{(-\beta+\alpha)^3} \\ 0 & 0 & 0 & \frac{\alpha\beta^2}{(-\beta+\alpha)^2} \\ \frac{\alpha^2\beta}{(-\beta+\alpha)^2} & \frac{(\alpha-3\beta)\alpha^2}{(-\beta+\alpha)^3} & 0 & 0 \\ 0 & \frac{\alpha^2\beta}{(-\beta+\alpha)^2} & 0 & 0 \end{bmatrix}. \quad (26)$$

We can now compute the matrix $M = q(\infty)^t q_J(\infty)^{-t}$ and the Meijer monodromy about the small radius point:

$$T[\infty] = MT_J[\infty]M^{-1}, \quad (27)$$

where:

$$T_J[\infty] = e^{2\pi i R_J[\infty]^t} = \begin{bmatrix} e^{-2i\pi\alpha} & 0 & 0 & 0 \\ 2i\pi e^{-2i\pi\alpha} & e^{-2i\pi\alpha} & 0 & 0 \\ 0 & 0 & e^{-2i\pi\beta} & 0 \\ 0 & 0 & 2i\pi e^{-2i\pi\beta} & e^{-2i\pi\beta} \end{bmatrix}. \quad (28)$$

3.3 The model $\mathbb{P}^5[3, 3]$

The mirror Y of this model can be realized as an orbifold ⁵ of a complete intersection $p_1 = p_2 = 0$ of two cubics in \mathbb{P}^5 :

$$\begin{aligned} p_1 &= x_1^3 + x_2^3 + x_3^3 - 3\psi x_4 x_5 x_6 \\ p_2 &= x_4^3 + x_5^3 + x_6^3 - 3\psi x_1 x_2 x_3. \end{aligned}$$

⁵We refer the reader to [22] for details about the orbifold action in this case.

The fundamental period and special coordinate in this example are discussed in [22, 18]. Reference [22] also discusses the counting of holomorphic curves for this model.

In this example, the hypergeometric coordinate is given by $z = \frac{1}{\psi^6}$. The matrices $R_{can}[\infty]$, $R_J[\infty]$ and a choice for the matrix P are given in Appendix A. This data allows us to compute the Meijer monodromies:

$$T[0] = \begin{bmatrix} 1 & 0 & 0 & 0 \\ -2i\pi & 1 & 0 & 0 \\ -4\pi^2 & -2i\pi & 1 & 0 \\ 0 & 0 & -2i\pi & 1 \end{bmatrix}, \quad T[\infty] = \begin{bmatrix} 1 & 0 & 0 & 0 \\ -5 & -3\frac{i}{\pi} & 9/4\pi^{-2} & \frac{9}{8}\frac{i}{\pi^3} \\ 10 & 15/2\frac{i}{\pi} & -\frac{27}{4}\pi^{-2} & -9/2\frac{i}{\pi^3} \\ -8 & -9\frac{i}{\pi} & \frac{27}{4}\pi^{-2} & \frac{27}{4}\frac{i}{\pi^3} \end{bmatrix} \quad (29)$$

and $T[1] = T[0]^{-1}T[\infty]$. These monodromy matrices satisfy:

$$(T[0] - I)^4 = 0 \quad , \quad (T[1] - I)^2 = 0 \quad , \quad (T[\infty]^3 - I)^2 = 0 \quad . \quad (30)$$

A set of periods associated with with a basis of a full sublattice of the integral lattice $H_3(Y, \mathbb{Z})$ (up to a *common* factor) is given by:

$$U_E(z) = EU(z) \quad , \quad \text{with} \quad E = \begin{bmatrix} 1 & 0 & 0 & 0 \\ -5 & -3\frac{i}{\pi} & 9/4\pi^{-2} & \frac{9}{8}\frac{i}{\pi^3} \\ 10 & 15/2\frac{i}{\pi} & -\frac{27}{4}\pi^{-2} & -9/2\frac{i}{\pi^3} \\ -8 & -9\frac{i}{\pi} & \frac{27}{4}\pi^{-2} & \frac{27}{4}\frac{i}{\pi^3} \end{bmatrix} . \quad (31)$$

It is also easy to check that the period $U_v(z) = \frac{3}{\pi^3} \left[\frac{3}{8}U_3 - \pi^2U_1 \right]$ vanishes at $z = 1$. This period is weakly integral since:

$$U_v(z) = -i[3, 3, 2, 1]U_E(z) \quad . \quad (32)$$

The relation $U_v(1) = 0$ is equivalent with an arithmetic identity which we write down in the Appendix.

In this case, the constant $\kappa = e^{2\psi(\alpha)+2\psi(\beta)-4\psi(1)} = \frac{1}{729} = 3^{-6}$ and the imaginary part of the algebraic coordinate on the moduli space is $s = -\frac{1}{2\pi} \log(\kappa|z|) = \frac{3}{\pi} \log\left(\frac{3}{|z|}\right)$. Figure 3 displays the values of $|U_v|$ versus s . The point $z = 1$ corresponds to $s = \frac{3 \log 3}{\pi} \approx 1.049$. For comparison, we also display the absolute values of the weakly integral period $\frac{9}{4\pi^2}U_2$ and of the special coordinate t . Figure 4 shows the absolute value of the special coordinate $t = -\frac{1}{2\pi i} \frac{U_1}{U_0}$ as a function of s , for $s \in [-6, 2]$. The asymptotic form of t in the small radius limit $z \rightarrow \infty$ can be easily computed from the small radius expansions given above:

$$t \approx -\frac{2(i\sqrt{3} \log(z) + (1+i)\pi)}{\sqrt{3}(-1+i\sqrt{3}) \log z} + O((\log z)^{-2}) = \frac{9 \log 3 - 6\pi s - 3i\sqrt{3} \log 3 + i\pi(\sqrt{3}s - 2)}{6(-3 \log 3 + \pi s)} + O(s^{-2}) .$$

In particular, the value of t in the limit $z = \infty$ is:

$$t_{lim} = -\frac{1}{2} + i\frac{\sqrt{3}}{6} \implies |t_{lim}| = \frac{1}{\sqrt{3}} \approx .577 \quad . \quad (33)$$

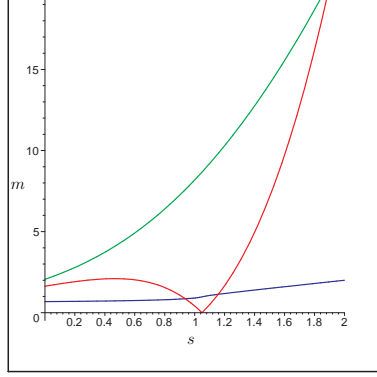


Figure 3. Graph of $|U_v|$, $\frac{9}{4\pi^2}|U_2|$ and $|t|$ versus the imaginary part s of the algebraic coordinate for $s \in [0, 2]$. The point $z = 1$ corresponds to $s = \frac{3\log 3}{\pi} \approx 1.049$.

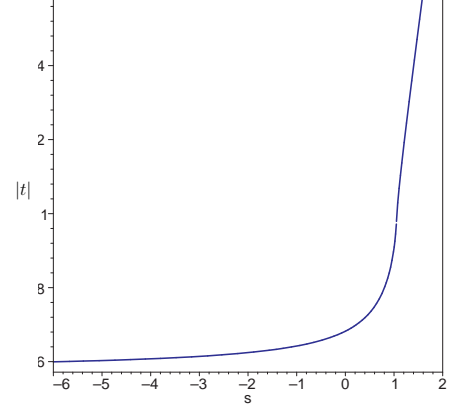


Figure 4. Graph of $|t|$ versus s for $s \in [-6, 2]$.

4 The family $\alpha_1 = \alpha_2 = \alpha_3 = \alpha_4$

In this section we consider the family (3), associated with the hypergeometric symbol $\left(\begin{smallmatrix} \alpha, \alpha, \alpha, \alpha \\ 1, 1, 1 \end{smallmatrix} \right)$, i.e. to the parameters $\alpha_1 = \alpha_2 = \alpha_3 = \alpha_4 = \alpha$, where we take $0 < \alpha < 1$ for simplicity. The hypergeometric equation of this family has the form:

$$\left[\delta^4 - z(\delta + \alpha)^4 \right] u = 0 \quad . \quad (34)$$

4.1 The Meijer periods

The expansion of the Meijer periods for $|z| < 1$ follows from the general results of Section 2, while the expansion for $|z| > 1$ is obtained by closing the contour to the right and applying the residue theorem. This brings contributions from the quadruple poles $s = -n - \alpha$, with n a nonnegative integer. In this case, the computation is rather similar to that leading to the large radius expansions (9), giving the result:

$$U_j(z) = \frac{1}{6} \left(\frac{\sin \pi \alpha}{\pi} \right)^{3-j} ((-1)^{j+1} z)^{-\alpha} \sum_{n=0}^{\infty} \left[\frac{(\alpha)_n}{n!} \right]^4 \mu_j(n, z) z^{-n} \quad , \quad (35)$$

where the quantities $\mu_j(n, z)$ are defined through:

$$\mu_j(n, z) = \xi_j''(-n-\alpha) + 3\xi_j'(-n-\alpha) (\xi_j(-n-\alpha) + i\pi\delta_{j,even} + \log z) + (\xi_j(-n-\alpha) + i\pi\delta_{j,even} + \log z)^3 \quad , \quad (36)$$

with:

$$\xi_j^{(i)}(-n-\alpha) = 4 \left[\psi^{(i)}(1) + i! \sum_{k=1}^n \frac{1}{k^{i+1}} \right] - (-1)^i (j+1) \psi^{(i)}(n+\alpha) - (3-j) \psi^{(i)}(1-n-\alpha) \quad (37)$$

for $i = 0, 1, 2$.

4.2 Meijer monodromies

The monodromies of the Meijer basis can be extracted by a procedure very similar to the one employed above. For the benefit of the reader interested in reproducing our computations, let us mention that in this case the correct row vector needed for extracting the singular behaviour around $z = \infty$ is:

$$Z = \begin{bmatrix} z^{-\alpha} & z^{-\alpha} \log(z) & z^{-\alpha} \log(z)^2 & z^{-\alpha} \log(z)^3 \end{bmatrix} \quad (38)$$

and that writing $U^t(z) = Z(z)q(z)$ produces a regular matrix function $q(z)$ whose value $q(\infty)$ at the point of interest has entries:

$$q_{ij}(\infty) = \frac{1}{6} \left(\frac{\sin \pi \alpha}{\pi} \right)^{3-j} (\delta_{j,odd} + \delta_{j,even} e^{-i\pi\alpha}) v_{ij}(\infty) \quad , \quad (39)$$

where:

$$\begin{aligned} v_{0j}(\infty) &= \xi_j''(-\alpha) + 3\xi_j'(-\alpha) (\xi_j(-\alpha) + i\pi\delta_{j,even}) + (\xi_j(-\alpha) + i\pi\delta_{j,odd})^3 \quad , \quad v_{3j}(\infty) = 1 \quad . \\ v_{1j}(\infty) &= 3\xi_j'(-\alpha) + 3(\xi_j(-\alpha) + i\pi\delta_{j,even})^2 \quad , \quad v_{2j}(\infty) = 3(\xi_j(-\alpha) + i\pi\delta_{j,odd}) \quad . \end{aligned}$$

(Here $\xi_j^{(i)}(-\alpha)$ are obtained from (37) by setting $n = 0$.)

The canonical and Jordan forms of the matrix $R[\infty]$ are:

$$R_{can}[\infty] = \begin{bmatrix} 0 & -1 & 0 & 0 \\ 0 & 0 & -1 & 0 \\ 0 & 0 & 0 & -1 \\ \alpha^4 & -4\alpha^3 & 6\alpha^2 & -4\alpha \end{bmatrix} \quad , \quad R_J[\infty] = \begin{bmatrix} -\alpha & 1 & 0 & 0 \\ 0 & -\alpha & 1 & 0 \\ 0 & 0 & -\alpha & 1 \\ 0 & 0 & 0 & -\alpha \end{bmatrix} \quad (40)$$

while a choice for the matrix P which defines a Jordan basis is:

$$P = \begin{bmatrix} \alpha^3 & \alpha^2 & \alpha & 1 \\ \alpha^4 & 0 & 0 & 0 \\ \alpha^5 & -\alpha^4 & 0 & 0 \\ \alpha^6 & -2\alpha^5 & \alpha^4 & 0 \end{bmatrix} \quad . \quad (41)$$

The matrix $q_J(z)$ is expressed in terms of the nilpotent orbit $S(z)$ of $\Phi_J(z)$ via:

$$q_J(z) = \begin{bmatrix} S_{1,1}(z) & S_{1,2}(z) & S_{1,3}(z) & S_{1,4}(z) \\ 0 & S_{1,1}(z) & S_{1,2}(z) & S_{1,3}(z) \\ 0 & 0 & 1/2S_{1,1}(z) & 1/2S_{1,2}(z) \\ 0 & 0 & 0 & 1/6S_{1,1}(z) \end{bmatrix} \xrightarrow{(S(\infty) = P)} q_J(0) = \begin{bmatrix} \alpha^3 & \alpha^2 & \alpha & 1 \\ 0 & \alpha^3 & \alpha^2 & \alpha \\ 0 & 0 & 1/2\alpha^3 & 1/2\alpha^2 \\ 0 & 0 & 0 & 1/6\alpha^3 \end{bmatrix} \quad .$$

Finally, the Meijer monodromy about $z = \infty$ can be computed as $T[\infty] = MT_J[\infty]M^{-1}$, where $M = q(0)^t q_J(0)^{-t}$ and:

$$T_J[\infty] = \begin{bmatrix} e^{-2\pi i \alpha} & 0 & 0 & 0 \\ 2\pi i e^{-2\pi i \alpha} & e^{-2\pi i \alpha} & 0 & 0 \\ -2\pi^2 e^{-2\pi i \alpha} & 2i\pi e^{-2\pi i \alpha} & e^{-2\pi i \alpha} & 0 \\ -\frac{4i\pi^3}{3} e^{-2\pi i \alpha} & -2\pi^2 e^{-2\pi i \alpha} & 2\pi i e^{-2\pi i \alpha} & e^{-2\pi i \alpha} \end{bmatrix} \quad . \quad (42)$$

The expression of the special coordinate (19) as a function of z follows easily from the small and large radius expansions of the Meijer periods. For later reference, we write down the form of $t(z)$ in the region $|z| > 1$:

$$t(z) = \frac{ie^{i\pi\alpha}}{2\sin\pi\alpha} \frac{\sum_{n=0}^{\infty} \left[\frac{(\alpha)_n}{n!}\right]^4 \mu_1(n, z) z^{-n}}{\sum_{n=0}^{\infty} \left[\frac{(\alpha)_n}{n!}\right]^4 \mu_0(n, z) z^{-n}} . \quad (43)$$

This allows us to extract the asymptotic form of t for $z \rightarrow \infty$:

$$t_{as} = \frac{ie^{i\pi\alpha}}{2\sin\pi\alpha} \frac{\mu_1(0, z)}{\mu_0(0, z)} = \frac{ie^{i\pi\alpha}}{2\sin\pi\alpha} \left[1 + \frac{3(\psi(\alpha) - \psi(1-\alpha) - i\pi)}{\log z} \right] + O((\log z)^{-2}) , \quad (44)$$

where we used the relations:

$$\xi_0(-\alpha) = 4\psi(1) - \psi(\alpha) - 3\psi(1-\alpha) , \quad \xi_1(-\alpha) = 4\psi(1) - 2\psi(\alpha) - 2\psi(1-\alpha) .$$

4.3 The model $\mathbb{P}^7[2, 2, 2, 2]$

The mirror of this model is given by an orbifold Y of the complete intersection $\{p_1 = p_2 = p_3 = p_4 = 0\}$, where:

$$\begin{aligned} p_1 &= x_1^2 + x_2^2 - 2\psi x_3 x_4 \\ p_2 &= x_3^2 + x_4^2 - 2\psi x_5 x_6 \\ p_3 &= x_5^2 + x_6^2 - 2\psi x_7 x_8 \\ p_4 &= x_7^2 + x_8^2 - 2\psi x_1 x_2 . \end{aligned} \quad (45)$$

The fundamental period of this example was determined in [18] (see also [22]), while the semiclassical structure of the Kähler moduli space was analyzed in detail in [23] by making use of the linear sigma model technology of [28]. Our techniques allow us to go further and perform a systematic analysis of all periods. In Section 5, we will use the results derived below in order to address certain puzzles about the small radius limit of this model.

In this example, ψ is related to the hypergeometric coordinate through $z = \psi^{-8}$. The associated hypergeometric symbol is $\left(\begin{matrix} 1/2, 1/2, 1/2, 1/2 \\ 1, 1, 1 \end{matrix} \right)$, so the model fits into the scheme discussed above for the particular value $\alpha = 1/2$. The canonical and Jordan forms of the monodromy about $z = \infty$, as well as a choice for the matrix P are given in Appendix A, while the Meijer monodromies are given by:

$$T[0] = \begin{bmatrix} 1 & 0 & 0 & 0 \\ -2i\pi & 1 & 0 & 0 \\ -4\pi^2 & -2i\pi & 1 & 0 \\ 0 & 0 & -2i\pi & 1 \end{bmatrix} , \quad T[\infty] = \begin{bmatrix} -7 & -4\frac{i}{\pi} & 4\pi^{-2} & 2\frac{i}{\pi^3} \\ -2i\pi & 1 & 0 & 0 \\ -4\pi^2 & -2i\pi & 1 & 0 \\ 0 & 0 & -2i\pi & 1 \end{bmatrix} , \quad (46)$$

and $T[1] = T[0]^{-1}T[\infty]$. These matrices satisfy:

$$(T[0] - I)^4 = 0 \quad , \quad (T[1] - I)^2 = 0 \quad , \quad (T[\infty]^2 - I)^4 = 0 \quad . \quad (47)$$

Note that the matrix $T[\infty]$ is *not* maximally unipotent.

Partial information about the integral structure is provided by a set of periods associated (up a *common factor*) with a basis of a full sublattice of $H_3(Y, \mathbb{Z})$:

$$U_E(z) = EU(z) \quad , \quad \text{with} \quad E = \begin{bmatrix} 1 & 0 & 0 & 0 \\ -7 & -4\frac{i}{\pi} & 4\pi^{-2} & 2\frac{i}{\pi^3} \\ 25 & 16\frac{i}{\pi} & -20\pi^{-2} & -12\frac{i}{\pi^3} \\ -63 & -44\frac{i}{\pi} & 56\pi^{-2} & 38\frac{i}{\pi^3} \end{bmatrix} . \quad (48)$$

In this case, one obtains two weakly integral periods vanishing at $z = 1$:

$$\begin{aligned} U_{v1} &= \frac{2i}{\pi^3}[U_3 - 2\pi^2 U_1] = [5, 6, 4, 1]U_E \quad , \\ U_{v2} &= -\frac{8}{\pi^2}[U_2 + i\pi U_1 - 2\pi^2 U_0] = [15, 11, 5, 1]U_E \quad . \end{aligned} \quad (49)$$

In the mirror picture, these correspond to a $D6$ and a $D4$ -brane which become massless at $z = 1$. In fact, any linear combination of these periods will also vanish there, so we can for example also consider the vanishing period $U_{v1} + U_{v2}$, which in the mirror picture also corresponds to a collapsing $D6$ -brane. This situation will be discussed in more detail in Section 5.

In this example, the constant $\kappa = e^{4(\psi(\alpha) - \psi(1))}$ has the value $2^{-8} = \frac{1}{256}$. Figure 5 displays the absolute values of the special coordinate t and of the weakly integral periods U_{v1} , U_{v2} as functions of the imaginary part $s = \frac{4}{\pi} \log \frac{2}{|z|}$ of the algebraic coordinate on the moduli space. In Figure 6 we plot the absolute value of the special coordinate t as a function of s , including the region $s < 0$ of the moduli space, which has no classical analogue. In this example, we have $\psi(\alpha) = \psi(1 - \alpha) = \psi(1/2)$, so the asymptotic form of t for $|z| \rightarrow \infty$ is:

$$t_{as} = -\frac{1}{2} + \frac{3i\pi}{2 \log z} \quad . \quad (50)$$

In particular, $J = \text{Im}(t) \approx \frac{3}{2} \frac{\pi}{\log |z|}$ remains nonnegative for $|z| \gg 1$, as pointed out ⁶ in [23].

⁶The reader should note that the variable z used in equation (37) of [23] is the *inverse* of the hypergeometric coordinate z used in the present paper.

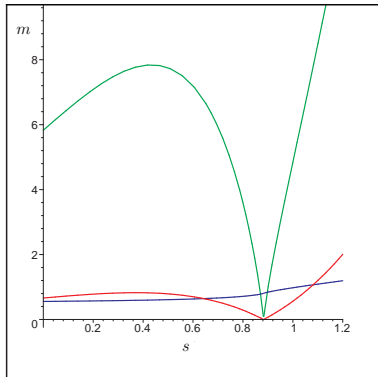


Figure 5. Graph of $|U_{v1}|$, $|U_{v2}|$ and $|t|$ versus the imaginary part s of the algebraic coordinate for $s \in [0, 1.2]$. The point $z = 1$ corresponds to $s = \frac{4 \log 2}{\pi} \approx 0.882$.

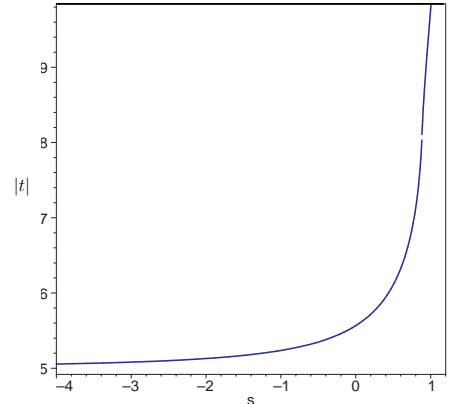


Figure 6. Graph of $|t|$ versus s for $s \in [-4, 1.2]$.

5 Small/large radius duality

5.1 Basic considerations

The results we have obtained for the model $\mathbb{P}^7[2, 2, 2, 2]$ apparently preclude us from interpreting $z = \infty$ as a large complex structure point. Indeed, the associated monodromy matrix is not maximally unipotent, but rather satisfies $(T[\infty]^2 - I)^4 = 0$. This behaviour is due to the factors of $z^{-\alpha} = z^{-1/2}$ in the expansions (35) of the periods for $|z| > 1$. One may be tempted to interpret this result as showing that the limit $z \rightarrow \infty$ of the model does not admit a standard geometric (i.e. Calabi-Yau) description [23]. However, the form of the monodromy about $z = \infty$ is tantalizingly close to that of the monodromy about a large complex structure point, which is an indication that something more interesting may be going on.

Indeed, it was noticed in [18] that the moduli space of this model admits a symmetry $z \rightarrow 1/z$. This follows by replacing ψ with its inverse and performing the change of coordinates:

$$\begin{aligned} x_1 &= y_1 + iy_2, & x_2 &= iy_1 + y_2 \\ x_3 &= y_7 + iy_8, & x_4 &= iy_7 + y_8 \\ x_5 &= y_5 + iy_6, & x_6 &= iy_5 + y_6 \\ x_7 &= y_3 + iy_4, & x_8 &= iy_3 + y_4 \end{aligned}, \tag{51}$$

which preserves the form of the defining equations (45). Hence the manifolds Y_ψ and $Y_{\frac{1}{\psi}}$ described by (45) for the parameters ψ and $\frac{1}{\psi}$ are isomorphic, which implies that the nature of the points $z = 0$ and $z = \infty$ is identical. Indeed, the isomorphism between

Y_ψ and $Y_{\frac{1}{\psi}}$ forces us to conclude that the points $z = 0$ and $z = \infty$ are physically indistinguishable — this is an *exact* statement in the full IIB string theory on Y , since its vector multiplet moduli space does not receive quantum corrections [46]. This, however, seems to be at odds with the different behaviour of the Meijer periods in the two limits $z = 0$ and $z = \infty$.

In order to clarify the situation, let us consider the effect of the change of variable $z \rightarrow s := 1/z$ on the hypergeometric equation (34). Under this operation, the equation is transformed into:

$$\left[s\delta'^4 - (\delta' - \alpha)^4 \right] \tilde{u}(s) = 0 \quad , \quad (52)$$

where $\delta' = s\frac{d}{ds} = -z\frac{d}{dz}$ and $\tilde{u}(s) := u(1/s)$. Thus (34) is *not* invariant under this symmetry. However, it is not hard to see that the form of (34) is preserved under the *combined* change of variable and function:

$$\begin{aligned} z &\rightarrow s := \frac{1}{z} \\ u &\rightarrow u' := z^{-\alpha}u \quad , \end{aligned} \quad (53)$$

i.e. $u(z) \rightarrow z^{-\alpha}u(1/z)$. Since $u(z) = \int_\gamma \Omega(z)$ is the period of the holomorphic 3-form Ω on a 3-cycle $\gamma \in H_3(Y, \mathbb{Z})$, it follows that the implementation of the symmetry $z \rightarrow \frac{1}{z}$ requires a rescaling of Ω :

$$\Omega(z) \rightarrow z^{-\alpha}\Omega(1/z) \quad . \quad (54)$$

What, then, is the correct interpretation of the point $z = \infty$? The answer follows by recalling that the moduli space of the closed conformal field theory on Y is built by considering marginal deformations, a process which is analytic in the deformation parameter z . This forces the periods to have different behavior in the regions $|z| < 1$ and $|z| > 1$. There is, however, a basic point to take into account: when performing marginal deformations one must specify a starting point ! In fact, one could as well choose this point to be $z = \infty$ and use the periods $\tilde{U}_j(z) = U_j(1/z)$ instead of $U_j(z)$. Therefore, the interpretation of $z = 0$ and $z = \infty$ as “large” and “small” radius points is indeed conventional and can be reversed, even though the analytic continuations of the associated periods do not coincide. In fact, interchanging these points corresponds to starting on different branches of a double cover of the moduli space. This follows by noticing that, since Y_z and $Y_{\frac{1}{z}}$ are isomorphic, the complex structure moduli space of Y is not the copy of \mathbb{P}^1 parameterized by z , but rather its quotient \mathcal{M} via this identification. This quotient is again a \mathbb{P}^1 , which can be parameterized, for example, by the variable:

$$x = \frac{2z}{z^2 + 1} \quad . \quad (55)$$

The map $z \rightarrow u$ gives a double cover of \mathcal{M} , branched over the points $x = +1$ and $x = -1$, which are the images of $z = 1$ and $z = -1$, respectively. The unit circle $|z| = 1$ is mapped into the region $x \in [-\infty, -1] \cup [1, \infty]$, which represents a segment on the associated Riemann sphere (see Figure 7). The points $z = 0$ and $z = \infty$ are both

mapped into the point $x = 0$. Since these points lie on different branches of our double cover, picking one of them as the large complex structure limit amounts to choosing a particular realization of the model.

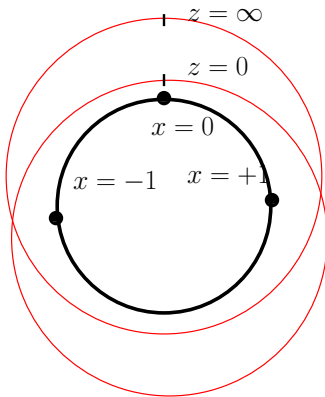


Figure 7. The coordinate z parameterizes a double cover of the complex structure moduli space of Y . The figure shows the topology of the restriction of this cover above the circle $\text{Im}(x) = 0$ on the Riemann sphere of x .

This situation is similar to the standard interpretation of T-duality for the conformal field theory on a circle. In that case, marginal deformations starting from a point $R > R_0$ build the continuation of the theory through the self-dual point $R_0 = \sqrt{\alpha'}$, into the region $R < R_0$. The duality $R \approx \tilde{R} = \alpha'/R$ identifies this continued theory with its form at a radius $\tilde{R} > R_0$, but this discrete identification is not captured by the marginal deformations. Just as in the case of T-duality, the global identification $z \approx 1/z$ in our model is “accidental” in the sense that it is not captured by marginal deformations associated with the (c, c) ring.

In order to make this more precise, let us compute the action of our symmetry on $H^3(Y, \mathbb{C})$. Consider acting with the transformation (53) on the Meijer periods:

$$U_j(z) \rightarrow U'_j(z) = z^{-1/2} U_j(1/z) \quad . \quad (56)$$

Since (53) is a symmetry of (34), it follows that both $(U_j)_{j=0..3}$ and $(U'_j)_{j=0..3}$ give a basis of solutions. Hence there must exist a constant matrix $C = (c_{ij})_{i,j=0..3}$ such that $U'_i(z) = c_{ij} U_j(z)$. In fact, this conclusion is a bit too quick, since the functions U_j are multi-valued, so we must be careful to take the branch-cuts into account. The correct statement is that such a relation must hold on every open and connected subset V of the moduli space which does not intersect the cuts. In fact, the matrix C can depend

on V ⁷. Since the set $V_0 = \{|z| < 1\}$ does not contain any cuts (see Figure 2), it suffices to start by considering our relation in this region. Hence we define C to be the matrix associated with V_0 . Then performing a transformation $z \rightarrow 1/z$ shows that the matrix associated with the region $V_1 = \{|z| > 1\}$ is the inverse of C . Thus, we expect the relations:

$$\begin{aligned} z^{-1/2}U(1/z) &= CU(z) \quad , \quad \text{if } |z| < 1 \\ z^{-1/2}U(1/z) &= C^{-1}U(z) \quad , \quad \text{if } |z| > 1 \quad . \end{aligned} \quad (57)$$

In order to check these equalities and determine the matrix C , let us take z to be such that $|z| < 1$. Then $|\frac{1}{z}| > 1$ and we have:

$$U_j(z) = \frac{(-1)^j}{j!} \sum_{n=0}^{\infty} \left[\frac{(\frac{1}{2})_n}{n!} \right]^4 \nu_j(n, z) z^n \quad (58)$$

$$U'_i(z) = \frac{(\delta_{i,odd} - i\delta_{i,even})}{6\pi^{3-i}} \sum_{n=0}^{\infty} \left[\frac{(\frac{1}{2})_n}{n!} \right]^4 \mu_i(n, 1/z) z^n \quad . \quad (59)$$

Defining b_{ij} via:

$$c_{ij} = (-1)^j j! \frac{(\delta_{i,odd} - i\delta_{i,even})}{6\pi^{3-i}} b_{ij} \quad , \quad (60)$$

it suffices to compute the matrix $B = (b_{ij})_{i,j=0..3}$, which satisfies:

$$\mu_i(n, 1/z) = b_{ij} \nu_j(n, z) \quad . \quad (61)$$

Using the explicit form of these sequences given in (10,11) and (36,37), it is not very hard to show that the required matrix has the form:

$$B = \begin{bmatrix} -6i\pi^3 & 18\pi^2 & 3i\pi & -1 \\ 0 & 6\pi^2 & 0 & -1 \\ 0 & 12\pi^2 & 3i\pi & -1 \\ 0 & 0 & 0 & -1 \end{bmatrix} \quad , \quad (62)$$

which finally leads to the transition matrix of interest:

$$C = \begin{bmatrix} -1 & 3\frac{i}{\pi} & \pi^{-2} & -\frac{i}{\pi^3} \\ 0 & -1 & 0 & \pi^{-2} \\ 0 & 2i\pi & 1 & -\frac{i}{\pi} \\ 0 & 0 & 0 & 1 \end{bmatrix} \Rightarrow C^{-1} = \begin{bmatrix} -1 & -\frac{i}{\pi} & \pi^{-2} & \frac{i}{\pi^3} \\ 0 & -1 & 0 & \pi^{-2} \\ 0 & 2i\pi & 1 & -\frac{i}{\pi} \\ 0 & 0 & 0 & 1 \end{bmatrix} \quad . \quad (63)$$

The geometric interpretation of these results follows by writing the Meijer periods in the form:

$$U_j(z) = \int_{g_j(z)} \Omega(z) \quad , \quad (64)$$

⁷In mathematical parlance, C is a locally constant matrix -valued function defined on the moduli space with the branch-cuts removed.

where $g_j(z)$ ($j = 0..3$) is a basis of $H_3(Y_z, \mathbb{C})$. Following the general theory of variations of Hodge structure (see [29] for a review in the context of its applications to mirror symmetry), we take the classes g_j to be flat with respect to the Gauss-Manin connection on the moduli space ⁸. Here Ω is normalized such that $\lim_{z \rightarrow 0} U_0(z) = 1$. On the other hand, using the variable $s = 1/z$ and starting with $s = 0 \iff z = \infty$ as the large complex structure point (in which case the Picard Fuchs equation coincides with the equation obtained from (34) by substituting s for z) gives Meijer periods $\tilde{U}_j(s) = U_j(1/s)$, which can also be written in the form:

$$\tilde{U}_j(s) = \int_{\tilde{g}_j(s)} \tilde{\Omega}(s) \ , \quad (65)$$

where $\tilde{g}_j(s)$ is a flat basis of $H_3(Y, \mathbb{C})$ while $\tilde{\Omega}$ is the holomorphic 3-form on Y normalized via $\lim_{s \rightarrow 0} \tilde{U}_0(s) = 1$. Then (57) shows that:

$$\tilde{g}_i(z) \equiv C_{ij} g_j(z) \quad (66)$$

$$\tilde{\Omega}(z) \equiv z^{1/2} \Omega(z) \ , \quad (67)$$

for $|z| < 1$. It follows that C encodes the relation between the Meijer bases g_i and \tilde{g}_i of $H_3(Y, \mathbb{C})$ associated with the points $z = 0$ and $z = \infty$, while the rescaling by $z^{1/2}$ reflects the different normalization of Ω required by their interpretation as large complex structure points.

We can now shed more light on the vanishing periods at $z = 1$. Indeed, applying (57) at that point shows that the vector $U(1) = \begin{bmatrix} U_0(1) \\ U_1(1) \\ U_2(1) \\ U_3(1) \end{bmatrix}$ is an eigenvector of C with eigenvalue one:

$$(C - I)U(1) = 0 \ . \quad (68)$$

The kernel of the matrix $(C - I)$ is a two-dimensional subspace spanned by the row vectors ⁹:

$$\left[0, -2\pi^2, 0, 1 \right] \ , \quad \left[-2\pi^2, i\pi, 1, 0 \right]$$

⁸Usually one takes this connection to act on cohomology, but here we use Poincare duality to transport the local system from $H^3(Y)$ to $H_3(Y)$. Hence we think of $g_i(z)$ as being flat sections of a bundle with fiber $H_3(Y_z)$. Then $g_i(z)$ will be multivalued due to the nontrivial holonomy of the connection.

⁹The matrix C has eigenvalues -1 and $+1$, each of which have multiplicity two. However, it is easy to check that C is not diagonalizable. The reader may wonder why we do not apply relation (57) to the other fixed point $z = -1$ and try to obtain vanishing periods there via a similar argument. The reason is, of course, that -1 is a branch point for our analytic continuations, so that the limit of $U(z)$ at this point is not well-defined. While (57) holds in a directional limiting sense at $z = -1$ (no matter from what direction in the complement of the cut we approach that point), this does not imply vanishing of a period there since the limits of $U(z)$ and $U(1/z)$ are different as z approaches the value -1 (note that z and $1/z$ lie on different sides of the cut).

associated with the vanishing periods (49). This reproduces the result of Section 4 that this model admits a two dimensional subspace of periods which vanish at $z = 1$. It also shows that this somewhat unusual situation is a consequence of the “accidental” symmetry $z \rightarrow 1/z$.

5.2 Physical interpretation

5.2.1 The closed string sector

Let us consider the implications of these results for the bulk conformal field theory associated with our compactification. The B-model defined by Y contains chiral primary operators $\mathcal{O}^{p,p}$ which are in one to one correspondence with generators of the Hodge groups $H^{p,3-p}(Y)$. When computing correlators, we can replace $H^{p,3-p}(Y)$ with their holomorphic counterparts $\mathcal{H}^{p,3-p} = \mathcal{F}^{3-p} \cap \mathcal{W}_p$, where:

$$0 \subset \mathcal{F}^0 \subset \mathcal{F}^1 \subset \mathcal{F}^2 \subset \mathcal{F}^3 = H^3(X) \quad (69)$$

is the Hodge filtration and:

$$0 \subset \mathcal{W}_0 \subset \mathcal{W}_1 \subset \mathcal{W}_2 \subset \mathcal{W}_3 = H^3(Y) \quad (70)$$

is the “reduced” monodromy weight filtration associated with a large complex structure point (see Appendix A of [1] for a short explanation of this concept). Roughly, \mathcal{W}_j is the space of those periods which have \log^j leading behaviour near that point¹⁰. The monodromy filtrations can be easily determined by making use of the special logarithmic behaviour of the Meijer periods (see the expansions (9)): if $z = 0$ is treated as a large complex structure point, then we obtain a filtration \mathcal{W} which can be identified with the spaces of periods spanned by:

$$\mathcal{W}_0 = \langle U_0 \rangle, \mathcal{W}_1 = \langle U_0, U_1 \rangle, \mathcal{W}_2 = \langle U_0, U_1, U_2 \rangle, \mathcal{W}_3 = \langle U_0, U_1, U_2, U_3 \rangle. \quad (71)$$

On the other hand, treating $z = \infty$ as a large complex structure point gives:

$$\tilde{\mathcal{W}}_0 = \langle \tilde{U}_0 \rangle, \tilde{\mathcal{W}}_1 = \langle \tilde{U}_0, \tilde{U}_1 \rangle, \tilde{\mathcal{W}}_2 = \langle \tilde{U}_0, \tilde{U}_1, \tilde{U}_2 \rangle, \tilde{\mathcal{W}}_3 = \langle \tilde{U}_0, \tilde{U}_1, \tilde{U}_2, \tilde{U}_3 \rangle. \quad (72)$$

Hence (57) implies a nontrivial relation between $(\tilde{\mathcal{W}})$ and (\mathcal{W}) and thus between $\tilde{\mathcal{H}}^{p,3-p}(Y_z)$ and $\mathcal{H}^{p,3-p}(Y_z)$. It follows that our symmetry involves a “rotation” of the chiral primary operators $\mathcal{O}^{p,3-p}$.

¹⁰The vector space $\mathcal{H}^3(Y_z)$ can be identified with the space spanned by the vectors $w_j := \begin{bmatrix} U_j(z) \\ \delta U_j(z) \\ \delta^2 U_j(z) \\ \delta^3 U_j(z) \end{bmatrix}$.

Viewing w_j as a set of initial conditions for the Picard Fuchs equation at the point z further identifies this space with the space of solutions to (34).

5.2.2 The D-brane sector

The (BPS saturated) D-brane sector of our compactification can be realized by considering the open conformal field theory or, equivalently, by including boundary states. In the large complex structure limit of the IIB theory on Y , these correspond to special Lagrangian cycles C in Y . Hence given a boundary state we can associate to it the homology class $\gamma = [C]$ of the associated cycle and hence the corresponding period $\int_\gamma \Omega$. As we move away from this limit, the correspondence may be destroyed for some boundary states, due to the fact that the path we use for performing the marginal deformations could cross a marginal stability line [20]. On such a line, the associated special Lagrangian cycle is expected to suffer a splitting transition of the type discussed in [7, 8]. Since we do not have a proper understanding of marginal stability lines in this model, the conclusions we can derive regarding the behaviour of D-brane states are only tentative.

The most basic question about such states concerns the dimensionality of the type IIA D-brane on X mirror to a given IIB D-brane on Y . As discussed in [17, 16, 26], this is determined by the order of the logarithmic behaviour of the associated period in the large complex structure limit, i.e. by the smallest component of the monodromy weight filtration which contains that period. In our model, we have *two* points which can play the role of large complex structure points, and hence two monodromy weight filtrations (\mathcal{W}) and ($\tilde{\mathcal{W}}$). Thus the correspondence between the mirror D-brane states (and even their dimension) involves a nontrivial rotation of $H_{\text{even}}(X)$.

A rather dramatic effect of this type can be observed as follows. Suppose that we define the large radius/large complex structure limit to correspond to $z = 0$. Then consider a $D2$ -brane in the large radius limit on X , whose mirror $D3$ -brane is associated (up to a factor) with the period U_1 . Note that this period is weakly integral (i.e. proportional with the period of Ω over an *integral* homology class of Y). Now perform marginal deformations until we cross the circle $|z| = 1$, reaching a point z_0 which lies outside the unit disk. At this point, we have a boundary state (the deformation of the original D-brane state) in the conformal field theory associated with z_0 . Performing a duality transformation maps this theory into an equivalent conformal theory for which the large radius point correspond to $z = \infty$; this transformation will modify the associated period through the action of C^{-1} (and rescaling by $z_0^{1/2}$). Inspection of the matrix C^{-1} (equation (63)) shows that the associated period has \log^2 behaviour around $z = \infty$, and hence the mirror boundary state corresponds to a $D4$ -brane! In fact, choosing z_0 to be far away in the z -plane assures that we are in the large radius limit of the dual model, and hence the associated $D4$ -brane must correspond to a holomorphic 4-cycle on X . In other words, our duality seems to identify some $D2$ -brane states on X with $D4$ -branes. Of course, this surprising conclusion may be avoided if the path used for analytic continuation crosses a marginal stability curve, or if the homology class under consideration does not actually contain a special Lagrangian cycle.

5.3 Small versus large size

What is the action of our symmetry on the size of X ? The answer to this question depends on the precise definition of “size”. Let us first consider the nonlinear sigma model measure of [44], which was shortly reviewed in the introduction. Following [44], we can start with $z = 0$ as the large radius point and measure size by using the analytic continuation of the special coordinate $t(z)$. Then the symmetry $z \rightarrow 1/z$ identifies $t(z)$ with $\tilde{t}(z) := t(1/z)$. Eliminating z defines a map $\tilde{t} = f(t)$, which can be determined numerically and is plotted in Figure 8 for $|z|$ belonging to the interval $(1, 10^4)$ (\tilde{J} remains positive in this range, even though this is not obvious at the scale and from the viewing angle of this figure). We see that the duality indeed maps small into large distances — a conclusion which is now established at the *quantum* level. Figure 9 displays the values of $t(z)$ for $|z| \in (1, 10^8)$. Note that $J = \text{Im}(t)$ remains positive when $\text{Im}(z) \neq 0$.

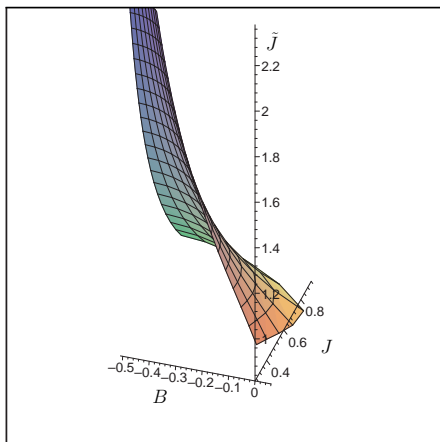


Figure 8. Graph of $\tilde{J} = \text{Im}(\tilde{t})$ vs $t = B + iJ$.

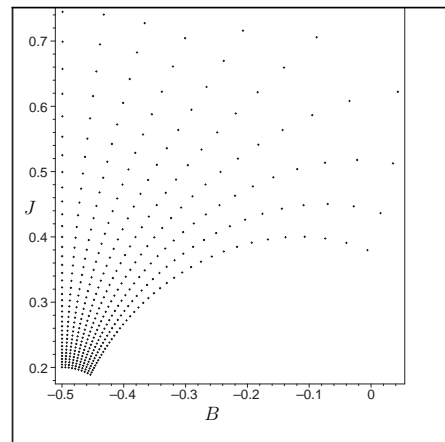


Figure 9. Values of $t(z)$ for $1 < |z| < 10^8$.

What about the quantum volume of X ? As discussed in the introduction, this is measured by the mass of a D6-brane wrapped over X , and it is natural to pick the D6-brane state whose mass vanishes at $z = 1$, which is plotted in Figure 5. There is no positive lower bound for the (quantum) volume of X — string theory allows the entire manifold to shrink to zero size.

5.4 Phases

The semiclassical Kahler moduli space of X was studied in [23], where it was shown that the model admits two phases, one of which is a large radius Calabi-Yau phase. The other phase can be analyzed via the linear sigma model techniques of [28], with the result that it is a hybrid phase which can be roughly described as a fibration of a \mathbb{Z}_2 Landau-Ginzburg orbifold over a \mathbb{P}^3 . This picture is tantalizingly close to a purely geometric description of that phase (say, in terms of a nonlinear sigma model having \mathbb{P}^3 or a closely related space as a target, for example through a construction along the lines of [33, 34, 35]) but, as pointed out in [23], the semiclassical picture provided by the linear sigma model is affected by strong quantum corrections which have the potential to seriously modify the discussion, thus making this geometric interpretation inconclusive. Our results allow us to make a precise statement about the effect of these corrections: they modify the theory in such a way that it becomes equivalent with its large radius incarnation ! In fact, once quantum corrections have been taken into account, there is no physical difference between the two limits and the model has a single phase (see Figure 10).

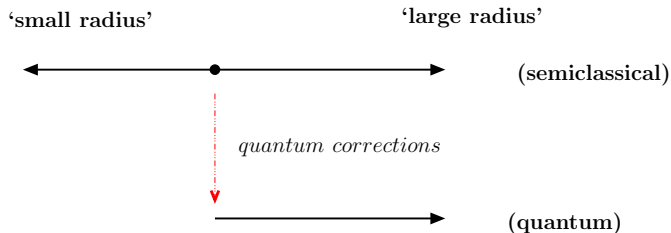


Figure 10. The effect of quantum corrections on the phase diagram of the IIA compactification on X .

5.5 Interpretation via special Lagrangian fibrations

How can we understand the behaviour of this model from the point of view of the SYZ conjecture [32] ?. Since both $z = 0$ and $z = \infty$ can be viewed as large complex structure points, the natural expectation is that Y_z should admit two special Lagrangian fibrations, well-defined on some vicinities of the points $z = 0$ and $z = \infty$, and related by the transformation (51). It was shown in [38, 40] that the monodromy weight filtration is determined by the fibration. Hence using one or the other of these fibrations corresponds to declaring $z = 0$ or $z = \infty$ to be the large complex structure point. Then our small-large radius duality appears as a consequence of the fact that the two fibrations are isomorphic.

The techniques for constructing special Lagrangian fibrations of Calabi-Yau manifolds are not yet fully developed (see [36, 37, 42, 38, 39, 40, 47] for partial results in this direction), so it is premature to attempt a complete analysis along these lines. However, simple and powerful methods are available in the large complex structure

limit [32, 42, 36, 40, 41], where the problem can be reduced to one of toric geometry and hence can be approached with the machinery available in such situations [15]. Appendix B uses a simple generalization of these techniques in order to identify the *topology* of the relevant fibrations. As in the hypersurface case, the base of each fibration turns out to be a 3-sphere.

The SYZ picture provides a natural interpretation of the nontrivial action of the duality on D-brane states: since mirror symmetry amounts to T-duality along the T^3 fibers, the dimension of the mirror D-brane depends on the relative position of a given IIB D3-brane with respect to the fibration of interest. Changing the fibration modifies this relative position, and hence can modify the dimension of the mirror holomorphic cycle. This is just the familiar fact that the dimension of a D-brane increases or decreases when performing T-duality along a direction orthogonal or parallel with its volume.

6 Conclusions

We completed the study of the hierarchy of one-parameter models introduced in [1], providing more evidence that the phenomena discussed in that paper are generic: in a typical IIA compactification on a one-parameter Calabi-Yau manifold, the non-perturbative state which becomes massless at the mirror of the conifold point is associated with a D6-brane. The general results derived in [1] and in the present paper should open the way for extensions of the work of [20] to more general Calabi-Yau compactifications, as well as providing a convenient framework for a systematic study of issues of marginal stability (see [20, 7, 8] for a few steps in this direction) through the effective field theory methods of [12].

From a methodological point of view, our results show that most one-parameter models fit into a hypergeometric hierarchy, which allows for a very systematic approach to the computation of all periods. This should help prepare the ground for further investigations of D-brane effects in Calabi-Yau compactifications. The universal large radius expansions we have obtained should also help clarify some of the arithmetic properties of the mirror map when combined with the work of [3] and [4].

We also performed a detailed study of a special one-parameter example, which displays some unusual features. In particular, we were able to bring some detailed evidence that this model realizes a Calabi-Yau version of large-small radius duality, thus confirming the suspicions of [18, 23]. We also presented evidence that, in the framework of [32], this duality is realized through the existence of *two* special Lagrangian fibrations — a feature which has interesting implications for the physics of D-branes in the associated string theory compactification. It would be interesting to investigate this phenomenon further, as well as its implications for the problem of marginal stability of D-brane states. Since the duality exchanges the small and radius points, it should be possible to use it in this model in order to extract strong results regarding this issue.

Another interesting question is to what extent these phenomena generalize. Multi-

ple large complex structure points are common in multi-parameter models (any model admitting topology-changing transitions possesses at least two such points). It would be interesting to see if similar discrete identifications occur in such models, and what can be learned from this about quantum corrections to the Kahler moduli space.

A Some intermediate results for the models $\mathbb{P}^5[3, 3]$ and $\mathbb{P}^7[2, 2, 2, 2]$

A.1 The model $\mathbb{P}^5[3, 3]$

The canonical and Jordan form of the matrix $R[\infty]$, as well as a choice for the matrix P are given below:

$$R_{can}[\infty] = \begin{bmatrix} 0 & -1 & 0 & 0 \\ 0 & 0 & -1 & 0 \\ 0 & 0 & 0 & -1 \\ \frac{4}{81} & -4/9 & \frac{13}{9} & -2 \end{bmatrix}, \quad R_J[\infty] = \begin{bmatrix} -2/3 & 1 & 0 & 0 \\ 0 & -2/3 & 0 & 0 \\ 0 & 0 & -1/3 & 1 \\ 0 & 0 & 0 & -1/3 \end{bmatrix}$$

$$P = \begin{bmatrix} 2/3 & 5 & 4/3 & -4 \\ 4/9 & 8/3 & 4/9 & -8/3 \\ \frac{8}{27} & 4/3 & \frac{4}{27} & -4/3 \\ \frac{16}{81} & \frac{16}{27} & \frac{4}{81} & -\frac{16}{27} \end{bmatrix}$$

The small radius arithmetic identity associated to the collapsing period at $z = 1$ is: $\sum_{n=0}^{\infty} \frac{a_n}{n!^2} = 0$, where

$$a_n = \Gamma(n + 1/3)^4 \Gamma(-n + 1/3)^2 \psi(-n + 1/3) + \Gamma(n + 1/3)^4 \Gamma(-n + 1/3)^2 \psi(n + 1) + \\ \Gamma(n + 2/3)^4 \Gamma(-n - 1/3)^2 \psi(-n - 1/3) + \Gamma(n + 2/3)^4 \Gamma(-n - 1/3)^2 \psi(n + 1) - \\ 2\Gamma(n + 1/3)^4 \Gamma(-n + 1/3)^2 \psi(-n + 2/3) - 2\Gamma(n + 2/3)^4 \Gamma(-n - 1/3)^2 \psi(-n + 1/3) .$$

A pair identity follows from the large radius expansions.

A.2 The model $\mathbb{P}^7[2, 2, 2, 2]$

In this case, we have:

$$R_{can}[\infty] = \begin{bmatrix} 0 & -1 & 0 & 0 \\ 0 & 0 & -1 & 0 \\ 0 & 0 & 0 & -1 \\ 1/16 & -1/2 & 3/2 & -2 \end{bmatrix}, \quad R_J[\infty] = \begin{bmatrix} -1/2 & 1 & 0 & 0 \\ 0 & -1/2 & 1 & 0 \\ 0 & 0 & -1/2 & 1 \\ 0 & 0 & 0 & -1/2 \end{bmatrix}$$

$$P = \begin{bmatrix} 1/8 & 1/4 & 1/2 & 1 \\ 1/16 & 0 & 0 & 0 \\ 1/32 & -1/16 & 0 & 0 \\ \frac{1}{64} & -1/16 & 1/16 & 0 \end{bmatrix}$$

B Special Lagrangian fibrations of Y

A topological T^3 fibration in the large complex structure limit can be obtained by the methods of [42]. This fibration is believed [32, 36, 40, 42] to admit a deformation to a

special Lagrangian fibration of Y as we move away from the large complex structure point. While the arguments discussed in those papers are restricted to hypersurfaces in toric varieties, our model $\mathbb{P}^7[2, 2, 2, 2]$ is more general since it is a complete intersection. Assuming that some generalization of those arguments goes through in our case, we can attempt to construct our fibration along the same lines.

For this, let us first consider the point $z = 0 \iff \psi = \infty$. In this limit, the defining equations (45) become:

$$\begin{aligned} x_1x_2 = 0 & \quad , & \quad x_3x_4 = 0 \\ x_5x_6 = 0 & \quad , & \quad x_7x_8 = 0 \quad , \end{aligned}$$

so that Y reduces to a union of 16 copies of \mathbb{P}^3 intersecting with normal crossings¹¹:

$$Y_\infty = \bigcup_{u_1, u_2, u_3, u_4 \in \mathbb{Z}_2} Z_{u_1, u_2, u_3, u_4} \quad , \quad (73)$$

where $Z_{u_1, u_2, u_3, u_4} = \{x = [x_1 \dots x_8] \in \mathbb{P}^7 \mid x_{1+u_1} = x_{3+u_2} = x_{5+u_3} = x_{7+u_4} = 0\} \approx \mathbb{P}^3$. Following the procedure of [42, 36, 40, 41], we consider the map $\mu : \mathbb{P}^7 \rightarrow \mathbb{R}^7$ given by:

$$\mu(x) = \frac{\sum_{k=1}^8 |x_k|^2 P_k}{\sum_{k=1}^8 |x_k|^2} \quad , \quad (74)$$

with $P_1 \dots P_8$ some points in general position in \mathbb{R}^7 . The convex hull of these points defines a 7-simplex denoted by Δ , which clearly coincides with the image of μ . According to the discussion of [42, 36, 40, 41], a candidate for the desired T^3 fibration of Y in the large radius limit is given by the restriction of μ to Y_∞ :

$$\mu_0 := \mu|_{Y_\infty} : Y_\infty \rightarrow \text{im}(\mu_0) \subset \Delta \quad . \quad (75)$$

Indeed, it is easy to see that the generic fiber of this map is a 3-torus. In the hypersurface case considered in [42, 36, 40, 41], the image of μ_0 coincides with the boundary of Δ (which is topologically a 3-sphere, since in the hypersurface case Δ has dimension 4), but for our complete intersection the situation is different. Indeed, it is easy to see that the image of each of the components Z is a three-dimensional face of Δ . For example, we have:

$$\mu(Z_{1,1,1,1}) = \left\{ \frac{|x_2|^2 P_2 + |x_4|^2 P_4 + |x_6|^2 P_6 + |x_8|^2 P_8}{|x_2|^2 + |x_4|^2 + |x_6|^2 + |x_8|^2} \mid (x_2, x_4, x_6, x_8) \in \mathbb{P}^3 \right\} \quad , \quad (76)$$

which coincides with the three dimensional face $\langle P_2, P_4, P_6, P_8 \rangle$ spanned by the vertices P_2, P_4, P_6 and P_8 . Hence the base of our fibration coincides with the union $\text{im}(\mu_0) = \Delta_0$ of 16 three-dimensional tetrahedra¹². These tetrahedra intersect along

¹¹In this appendix, Y_∞ and Y_0 mean $Y_{\psi=\infty}$ and $Y_{\psi=0}$, respectively.

¹² Δ_0 is a subset of (but does not coincide with) the 3-skeleton of Δ (i.e. the union of all of its three-dimensional faces).

common vertices, edges and facets, and the fibers of μ_0 degenerate at the points of intersection.

What is the topology of the base Δ_0 ? To answer this question, note that the 16 tetrahedra composing the base are spanned by the vertices:

$$\begin{aligned}
 &\langle 2, 4, 5, 8 \rangle \quad , \quad \langle 1, 4, 5, 8 \rangle \quad , \quad \langle 1, 4, 6, 8 \rangle \quad , \quad \langle 2, 4, 6, 8 \rangle \\
 &\langle 2, 4, 5, 7 \rangle \quad , \quad \langle 1, 4, 5, 7 \rangle \quad , \quad \langle 1, 4, 6, 7 \rangle \quad , \quad \langle 2, 4, 6, 7 \rangle \\
 &\langle 2, 3, 5, 7 \rangle \quad , \quad \langle 1, 3, 5, 7 \rangle \quad , \quad \langle 1, 3, 6, 7 \rangle \quad , \quad \langle 2, 3, 6, 7 \rangle \quad , \\
 &\langle 2, 3, 5, 8 \rangle \quad , \quad \langle 1, 3, 5, 8 \rangle \quad , \quad \langle 1, 3, 6, 8 \rangle \quad , \quad \langle 2, 3, 6, 8 \rangle
 \end{aligned}$$

and Δ_0 is obtained by gluing these along their common faces. Then a moment's thought shows that the resulting body is a 3-sphere (see Figures 11 and 12). Thus, just as in the hypersurface case, Y_∞ is a T^3 fibration over S^3 .

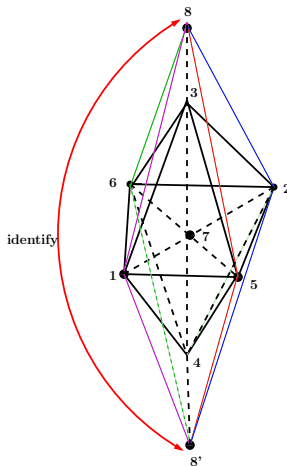


Figure 11. Arrangement of the 16 tetrahedra which form the base Δ_0 . The points 8 and 8' are identified, together with all identifications of edges and facets implied by this.

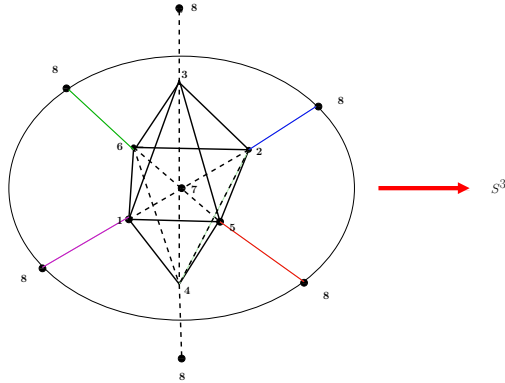


Figure 12. The identifications in Figure 11 can be performed in two steps. First, identify the edges starting from the point $P_8 \equiv P'_8$; we represent this by introducing 6 copies of that point. This shows that the topology of the base with the point P_8 removed is that of \mathbb{R}^3 . Identifying the 6 copies of P_8 amounts to adding a point to \mathbb{R}^3 , which can be thought of as “the point at infinity”. This produces a 3-sphere.

Let us now consider the limit $z \rightarrow \infty \iff \psi \rightarrow 0$. In this limit, the defining equations reduce to:

$$\begin{aligned} x_1^2 + x_2^2 = 0 & \quad , \quad x_3^2 + x_4^2 = 0 \\ x_5^2 + x_6^2 = 0 & \quad , \quad x_7^2 + x_8^2 = 0 \quad , \end{aligned}$$

which, via the transformation (51) are equivalent with:

$$\begin{aligned} y_1 y_2 = 0 & \quad , \quad y_3 y_4 = 0 \\ y_5 y_6 = 0 & \quad , \quad y_7 y_8 = 0 \quad . \end{aligned}$$

Hence Y_0 reduces once again to 16 copies of \mathbb{P}^3 intersecting transversely, as should be expected from the fact that Y_ψ and $Y_{1/\psi}$ are isomorphic as complex manifolds. Since the form of (77) is the same as above, we can once again use the map:

$$\tilde{\mu}(y) = \frac{\sum_{k=1}^8 |y_k|^2 Q_k}{\sum_{k=1}^8 |y_k|^2} \quad (77)$$

(with Q_k some points in general position in \mathbb{R}^7) in order to produce a T^3 -fibration $\tilde{\mu}_0$ of Y_0 whose basis is a 3-sphere.

The fibrations μ_0 and $\tilde{\mu}_0$ are related through the biholomorphic map $\phi : Y_\infty \rightarrow Y_0$ which identifies the complex structures J_∞ and J_0 of Y_∞ and Y_0 :

$$J_0 = d\phi \circ J_\infty \circ (d\phi)^{-1} \quad . \quad (78)$$

We may hope that some appropriate deformations of the fibrations μ_0 , $\tilde{\mu}_0$ are special Lagrangian with respect to J_∞ , J_0 and the associated metrics.

References

- [1] B. R. Greene, C. I. Lazaroiu, *Collapsing D-Branes in Calabi-Yau Moduli Space: I*, hep-th/0001025.
- [2] A. Klemm, E. Zaslow, *Local Mirror Symmetry at Higher Genus*, hep-th/9906046.
- [3] Bong H. Lian, Shing-Tung Yau, *Arithmetic Properties of Mirror Map and Quantum Coupling*, Commun.Math.Phys. 176 (1996) 163-192, hep-th/9411234.
- [4] Charles F. Doran *Picard-Fuchs Uniformization: Modularity of the Mirror Map and Mirror-Moonshine*, math.AG/9812162.
- [5] M. Gromov, *Pseudo-holomorphic curves on almost complex manifolds*, Invent. Math **82** (1985), 307–347.
- [6] E. Witten, *Topological sigma models*, Commun. Math. Phys **118** (1988), 411–449.
- [7] D. Joyce, *On counting special Lagrangian homology 3-spheres*, hep-th/9907013.
- [8] S. Kachru, J. McGreevy, *Supersymmetric Three-cycles and (Super)symmetry Breaking*, Phys. Rev. D61 (2000) 026001, hep-th/9908135.
- [9] J. Polchinski, A. Strominger, *New Vacua for Type II String Theory*, Phys. Lett. **B388** (1996) 736-742, hep-th/9510227.
- [10] C. Vafa, *Extending Mirror Conjecture to Calabi-Yau with Bundles*, hep-th/9804131.
- [11] M. Kontsevich, *Homological Algebra of Mirror Symmetry*, Proceedings of the International Congress of Mathematicians, (Zurich, 1994), 120–139, Birkhauser, alg-geom/9411018.
- [12] G. Moore, *Attractors and Arithmetic*, hep-th/9807056, *Arithmetic and Attractors*, hep-th/9807087.
- [13] P. S. Aspinwall, B. R. Greene, D. R. Morrison, *The Monomial-Divisor Mirror Map*, Internat. Math. Res. Notices (1993), 319-337, alg-geom/9309007.
- [14] D. R. Morrison, *Mirror symmetry and rational curves on quintic threefolds: a guide for mathematicians*, J. Amer. Math. Soc. **6** (1993) 223–247, alg-geom/9202004.
- [15] W. Fulton, *Introduction to toric varieties*, Annals of Mathematics Studies **131**, Princeton U.P., 1993; T. Oda, *Convex bodies and algebraic geometry: an introduction to the theory of toric varieties*, Ergebnisse der Mathematik und ihrer Grenzgebiete; 3.Folge, **15**, Springer, 1988; D. A. Cox, *Recent developments in toric geometry*, alg-geom/9606016.
- [16] B. R. Greene, Y. Kanter, *Small Volumes in Compactified String Theory*, Nucl. Phys. **B497** (1997) 127-145, hep-th/9612181.
- [17] H. Ooguri, Y. Oz, Z. Yin, *D-Branes on Calabi-Yau Spaces and Their Mirrors*, Nucl.Phys. **B477** (1996) 407-430, hep-th/9606112.

- [18] P. Berglund, P. Candelas, X. de la Ossa, A. Font, T. Hubsch, D. Jancic, F. Quevedo, *Periods for Calabi–Yau and Landau–Ginzburg Vacua*, Nucl.Phys. **B419** (1994) 352-403.
- [19] P. Candelas, X. C. De La Ossa, P. S. Green and P. Parkes, *A Pair of Calabi–Yau Manifolds as an Exactly Soluble Superconformal Theory*, Nucl. Phys. **B359** (1991) 21.
- [20] I. Brunner, M. R. Douglas, A. Lawrence, C. Romelsberger, *D-branes on the Quintic*, hep-th/9906200.
- [21] M. R. Douglas, *Topics in D-geometry*, hep-th/9910170.
- [22] A. Libgober, J. Teitelbaum, *Lines on Calabi–Yau complete intersections, mirror symmetry, and Picard–Fuchs equations*, Internat. Math. Res. Notices 1993, **no. 1**, 29–39.
- [23] P. S. Aspinwall, B. .Greene, *On the geometric interpretation of $N = 2$ superconformal theories*, Nucl. Phys. **B437** (1995) 205-230, hep-th/9409110.
- [24] O. I. Marichev, *Handbook of integral transforms of higher transcendental functions: theory and algorithmic tables*, Ellis Horwood series in mathematics and its applications, Halsted Press, New York 1983; A. Erdelyi, W. Magnus, F. Oberhettinger, F. G. Tricomi, *Higher transcendental functions*; Y. Luke, *The special functions and their approximations*, Academic Press, 1969.
- [25] D. R. Morrison, *Picard–Fuchs equations and mirror maps for hypersurfaces*, in Essays on mirror manifolds, 241–264, Internat. Press, Hong Kong, 1992, hep-th/9111025.
- [26] D. R. Morrison, *Mirror symmetry and the type II string*, Nucl. Phys. Proc. Suppl. **46** (1996) 146-155, hep-th/9512016.
- [27] N. E. Norlund, *Hypergeometric functions*, Acta Mathematica, **4** (1955), 289–349.
- [28] E. Witten, *Phases of $N = 2$ Theories In Two Dimensions*, Nucl. Phys. **B403** (1993) 159.
- [29] D. R. Morrison, *Mathematical aspects of Mirror Symmetry*, Complex Algebraic Geometry (J. Kollar, ed.), IAS/Park City Math. Series, vol. 3, 1997, pp. 265-340, alg-geom/9609021.
- [30] D. R. Morrison, *Compactifications of moduli spaces inspired by mirror symmetry*, Journées de Géométrie Algébrique d’Orsay (Juillet 1992), Astérisque, vol. **218**, 1993, pp. 243-271, alg-geom/9304007.
- [31] V. V. Batyrev, D. van Straten, *Generalized hypergeometric functions and rational curves on Calabi–Yau complete intersections in toric varieties*, Comm. Math. Phys. **168** (1995), no. 3, 493–533.
- [32] A. Strominger, S.-T. Yau, E. Zaslow, *Mirror Symmetry is T-Duality*, Nucl. Phys. **B479** (1996) 243-259, hep-th/9606040.

- [33] P. Candelas, E. Derrick, and L. Parkes, *Generalized Calabi-Yau Manifolds and the Mirror of a Rigid Manifold*, Nucl.Phys. **B407** (1993) 115–154.
- [34] R. Schimmrigk, *Critical Superstring Vacua from Noncritical Manifolds: A Novel Framework for String Compactification*, Phys. Rev. Lett. **70** (1993) 3688–3691.
- [35] S. Sethi, *Supermanifolds, Rigid Manifolds and Mirror Symmetry*, Nucl. Phys. **B430** (1994) 31–50.
- [36] W.-D. Ruan, *Lagrangian tori fibration of toric Calabi-Yau manifold I*, math.DG/9904012.
- [37] W.-D. Ruan, *Lagrangian Tori Fibration of Toric Calabi-Yau manifold III: Symplectic topological SYZ mirror construction for general quintics*, math.DG/9909126.
- [38] M. Gross, *Special Lagrangian Fibrations I: Topology*, alg-geom/9710006
- [39] M. Gross, *Special Lagrangian Fibrations II: Geometry*, math.AG/9809072 .
- [40] M. Gross, *Topological Mirror Symmetry*, math.AG/9909015.
- [41] N. C. Leung, C. Vafa, *Branes and toric geometry*, Adv.Theor.Math.Phys. **2** (1998) 91-118, hep-th/9711013.
- [42] I. Zharkov, *Torus Fibrations of Calabi-Yau Hypersurfaces in Toric Varieties and Mirror Symmetry*, math.AG/9806091.
- [43] P. S. Aspinwall, B. R. Greene, D. R. Morrison, *Calabi-Yau Moduli Space, Mirror Manifolds and Spacetime Topology Change in String Theory*, Nucl. Phys. **B416** (1994) 414–480; P. S. Aspinwall, B. R. Greene, D. R. Morrison, *Multiple Mirror Manifolds and Topology Change in String Theory*, Phys. Lett. **B303** (1993) 249–259
- [44] P. S. Aspinwall, B. R. Greene, D. R. Morrison, *Measuring small distances in $N=2$ sigma models*, Nucl. Phys. **B420** (1994) 184-242, hep-th/9311042.
- [45] P. Aspinwall, *Minimum Distances in Non-Trivial String Target Spaces*, Nucl.Phys. **B431** (1994) 78-96, hep-th/9404060.
- [46] B. de Wit, P. Lauwers, A. Van Proeyen, *Lagrangians of $N = 2$ supergravity-matter systems*, Nucl. Phys. **B255** (1985) 569–608; A. Strominger, *Massless Black Holes and Conifolds in String Theory*, Nucl. Phys. **B451** (1995) 96-108, hep-th/9504090.
- [47] N. Hitchin, *Lectures on special Lagrangian submanifolds*, math.DG/9907034.